IEEE Photonics Journal
An IEEE Photonics Society Publication

Open Access

Cost-Effective Mach-Zehnder Interferometer Liquid Refractive Index Sensor Based on Conventional Polymer Strip Waveguide

Volume 13, Number 1, February 2021

Xiao Xia Ma
Kai Xin Chen
Jie Yun Wu

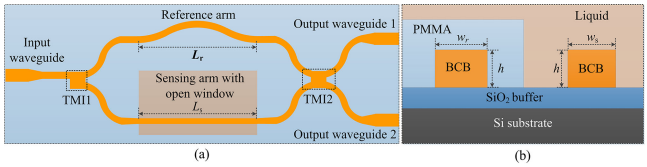

DOI: 10.1109/JPHOT.2020.3041731

Cost-Effective Mach-Zehnder Interferometer Liquid Refractive Index Sensor Based on Conventional Polymer Strip Waveguide

Xiao Xia Ma, Kai Xin Chen, and Jie Yun Wu

School of Optoelectronic Science and Engineering, University of Electronic Science and Technology of China, Chengdu 611731, China

DOI:10.1109/JPHOT.2020.3041731
This work is licensed under a Creative Commons Attribution 4.0 License. For more information, see https://creativecommons.org/licenses/by/4.0/

Manuscript received September 25, 2020; revised November 24, 2020; accepted November 28, 2020. Date of publication December 1, 2020; date of current version December 31, 2020. This work was supported in part by the National Natural Science Foundation of China under Grant 62075027 and U1533121, in part by the Key R&D Program of Sichuan Province under Grant 2020YFSY0003, in part by the Opened Fund of the State Key Laboratory of Integrated Optoelectronics under Grant IOSKL2018KF12, and in part by the Fundamental Research Funds for the Central Universities under Grant ZYGX2019J050. Corresponding author: Kai Xin Chen. (e-mail: chenkx@uestc.edu.cn).

Abstract: We propose and demonstrate a cost-effective liquid refractive index (RI) sensor in polymer materials by employing a Mach-Zehnder interferometer (MZI) formed with the conventional strip waveguide. The proposed sensor can attain high sensitivity by choosing a suitable reference arm length to reduce optical path difference (OPD) between the two arms of the employed MZI. Our fabricated devices, which have the same sensing arm length of 7900 μm but different reference arm lengths of 7900.0, 7942.5, 7950.9, 7962.2, and 7969.5 μm, respectively, exhibit the maximum RI sensitivities of 33662.8 nm/RIU, and almost the same detection range (DR) of 0.0041 ± 0.0002 RIU.

Index Terms: Liquid refractive index sensor, highly sensitive, Mach-Zehnder interferometer, optical path difference, strip waveguide.

1. Introduction

Over the past decades, optical waveguide liquid refractive index (RI) sensors have received more and more attention as an increasingly important tool in biochemical analysis applications by virtue of their unique advantage enabling high-sensitive, real-time, and label-free detection [1]. To date, various optical waveguide liquid RI sensors employing various configurations, including ring resonator [2]–[4], grating-assisted directional coupler [5], grating [6], Young interferometer [7], multimode interferometer [8], and Mach-Zehnder interferometer (MZI) [9]–[18], have been proposed. Among them, the MZI-based sensors have distinctive advantages of structural simplicity and diversity, design flexibility, and the potential of ultra-high sensitivity, making them an important and promising type.

Considering that the regeneration of the sensor after use is a very complicated and time-consuming procedure, it is much desired to develop low-cost and high sensitivity (i.e., cost-effective) liquid RI sensors. For the MZI-based sensors, the sensitivity is defined as the ratio of the variation of the output power (intensity interrogation) or the shift of the transmission spectra

(spectral interrogation) to the variation of the analyte RI, and determined mainly by the used waveguide structure and MZI configuration. As the MZI-based sensors also utilize evanescent field probing scheme, to enhance light-analyte interactions and hence to achieve large waveguide sensitivity, strong penetration of the evanescent field into the analyte is required. To this end, some novel waveguides, including plasmonic waveguide [10], slot waveguide [11], hybrid plasmonic waveguide [12],[13], subwavelength grating slot waveguide [14], and the waveguide with metal under-cladding [15], have been proposed and evaluated during the past years. And they actually help the improvement of the waveguide sensitivity. However, these novel waveguides also increase the complexity of the sensor design and fabrication and hence, the cost of the device in comparison with the conventional strip waveguide.

Generally, to enhance the sensitivity the reference arm of a MZI sensor is isolated from the analyte by covering suitable cladding layer, resulting in an asymmetric MZI configuration. As an interferometric device, optical path difference (OPD) between the two arms, determined by the configurations and the parameters of the employed asymmetric MZI, has significant impact on the sensitivity of the sensor. Especially, to pursue an ultra-high sensitivity, the OPD of the used MZIs in [16], [17] were designed carefully to induce the dip splitting effect in the transmission spectra at the critical working point. However, due to small fabrication tolerance of the devices, to attain good devices characteristics an accurate fabrication process with expensive facilities is required, resulting in a high cost. In addition, the cascaded MZI configuration has also been employed to introduce the Vernier effect to enhance the sensitivity [18]. But it also increases the sensor size as well as the design and fabrication complexity and hence, the cost of the device in comparison with the single MZI configuration.

The motivation of this work is to develop a cost-effective liquid RI sensor in polymer materials. To this end, a simple asymmetric MZI formed with the conventional strip waveguide is employed, in which the reference arm length and hence the OPD between the two arms is optimized to attain a high sensitivity. Meanwhile, a two-mode interferometer is introduced to balance the optical powers between the two arms so as to maximize the extinction ratio. Optical polymer is one of the most promising materials platforms for the implementation of a cost-effective liquid RI sensor because of the availability of a wide range of polymer material with controllable refractive index as well as simple waveguide fabrication process. Our theoretical results exhibit a ultra-high RI sensitivity of 9×10^4 nm/RIU for the proposed MZI sensor with a light-analyte interactive length of 7900.0 μm and a reference length of 7980.0 μm, which has a $\sim$17-fold enhancement in comparison with the sensitivity of 5264.0 nm/RIU, achieved by the MZI sensor with the same reference and sensing arm length of 7900.0 μm. Our fabricated five devices, which have the same light-analyte interactive length of 7900.0 μm but different reference arm lengths of 7900.0, 7942.5, 7950.9, 7962.2, and 7969.5 μm, exhibit the RI sensitivities of 5151.1, 10598.9, 12110.8, 24218.6 and 33662.8 nm/RIU, respectively, and almost the same detection range (DR) of 0.041 $\pm$ 0.002 RIU. These experimental results are in excellent agreement with the theoretical ones. Our proposed MZI sensor is cost-effective because of its structural simplicity, easy processing, and mass fabrication capability.

2. Principle and Design

The proposed MZI is shown schematically in Fig. 1(a), which is an asymmetric MZI configuration formed by two waveguide arms sandwiched between two two-mode interferometers (TMI1 and TMI2). The two arms of the MZI, corresponding to the sensing arm and the reference arm, have different physical length of L_{s} and L_{r}, respectively. TMI1 at the input end is used to distribute unevenly the input light into the reference and sensing arms, and more light power into the sensing arm to compensate the loss in this arm and therefore, maximize the extinction ratio. TMI2 at the output end is used to combine the two light beams from the two arms to acquire the optical interference. Four sections of identical S bends allowing a negligible bending loss are used to connect the two arms and the two TMIs, while two sections of identical S bends are used to connect the output TMI to the two output waveguides via two tapered straight waveguides. Another tapered straight waveguide is used to connect the input waveguide and the input TMI. To reduce the

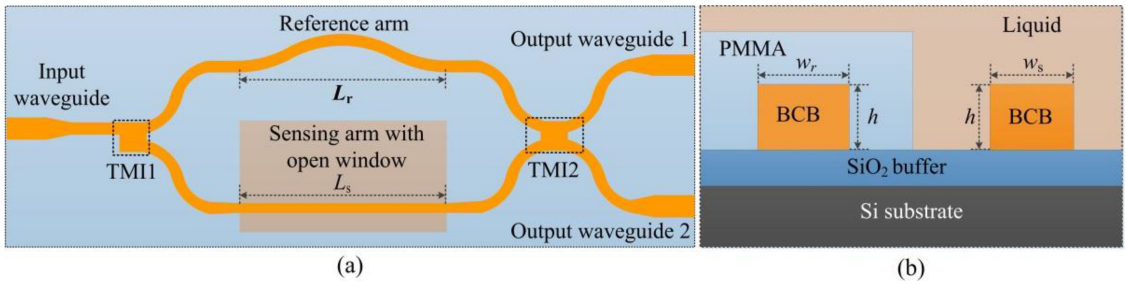

Fig. 1. Schematic diagram (a) and cross-sectional view of the two arms (b) of the proposed MZI sensor.

coupling loss between the fiber and the input/output waveguides, the width of the input and output waveguides are designed to be a little wider. The entire device is covered with a cladding layer except that the sensing arm with open window is exposed to the liquid analyte to be measured.

The cross-sectional view of the two arms of the proposed MZI together with the materials used in this work is shown schematically in Fig. 1(b). All involved waveguides employ conventional strip one, the core is polymer benzocyclobutene (BCB), the buffer silica (SiO_2), and the cladding polymethyl methacrylate (PMMA). The refractive indices of BCB, SiO_2 and PMMA are 1.5370, 1.4444 and 1.4710, respectively. The sensing window is filled with liquid analyte to be measured. In our design, the filled liquid is assumed to be DI water with RI of 1.3180 [19]. With these parameters, we design the two waveguide arms and the two TMI waveguides by solving the modes with a commercial mode solver (COMSOL). Considering that the larger the core of the waveguide, the smaller the loss, but the lower the waveguide sensitivity, thus to accommodate only the fundamental mode and meanwhile to balance the waveguide sensitivity and the propagation loss, the widths of the reference and sensing waveguide arms are designed carefully and the optimized widths are chosen to be $w_r = 2.5$ μm and $w_s = 2.0$ μm respectively, both with the same height of $h = 1.7$ μm. Meanwhile, to support the fundamental and the first-order modes, the two TMIs are designed to be with the same width of 6.0 μm but different lengths of 41.0 μm for TMI1 to achieve a power splitting ratio of ∼3:1 between the sensing and the reference arms and 25.5 μm for TMI2 to achieve the ratio of ∼1:1.

For the proposed MZI, the phase difference φ between the two arms can be expressed as:

$$\varphi = \frac{2\pi}{\lambda}[n_{eff}(r)L_r - n_{eff}(s)L_s] \tag{1}$$

where λ is the operating wavelength, $n_{eff}(i)$ $(i = r, s)$ is the effective index of the fundamental mode in the reference or the sensing waveguide arm. The proposed MZI has periodic transmission dips that correspond to destructive interference when the phase difference $\varphi = m\pi$, where m is an odd number. According to Eq. (1), the wavelengths λ_{dip} at these dips can be written as:

$$\lambda_{dip} = \frac{2}{m}[n_{eff}(r)L_r - n_{eff}(s)L_s] \tag{2}$$

A change in liquid concentration corresponds to a change Δn_l in the liquid analyte RI n_l, which results in a change $\Delta n_{eff}(s)$ in $n_{eff}(s)$ in the sensing waveguide arm, and hence the dip shift $\Delta\lambda_{dip}$ in the transmission spectrum of the MZI. In view of the wavelength dependence of the effective index, the wavelengths $\lambda_{\rm dip}+\Delta\lambda_{dip}$ at these new dips can be written as:

$$\lambda_{dip} + \Delta\lambda_{dip} = \frac{2}{m}\left[\left(n_{eff}(r) + \Delta\lambda_{dip}\frac{\partial n_{eff}(r)}{\partial\lambda}\right)L_r - \left(n_{eff}(s) + \Delta\lambda_{dip}\frac{\partial n_{eff}(s)}{\partial\lambda} + \Delta n_l\frac{\partial n_{eff}(s)}{\partial n_l}\right)L_s\right] \tag{3}$$

According to Eq. (2) and Eq. (3), $\Delta\lambda_{dip}$ can be expressed as:

$$\Delta\lambda_{dip} = \frac{2}{m}\left[\Delta\lambda_{dip}\frac{\partial n_{eff}(r)}{\partial\lambda}L_r - \left(\Delta n_l\frac{\partial n_{eff}(s)}{\partial n_l} + \Delta\lambda_{dip}\frac{\partial n_{eff}(s)}{\partial\lambda}\right)L_s\right] \tag{4}$$

Further, using Eq. (2) and Eq. (4) to cancel m, one can obtain

$$\frac{\Delta n_l}{\Delta \lambda_{dip}} \frac{\partial n_{eff}(s)}{\partial n_l} \lambda_{dip} L_s = \left[\left(n_{eff}(r) - \lambda_{dip} \frac{\partial n_{eff}(r)}{\partial \lambda} \right) L_r - \left(n_{eff}(s) - \lambda_{dip} \frac{\partial n_{eff}(s)}{\partial \lambda} \right) L_s \right] \tag{5}$$

Using

$$n_g(i) = n_{eff}(i) - \lambda \frac{\partial n_{eff}(i)}{\partial \lambda} \tag{6}$$

where n_g (i) ($i = r, s$) is the group effective index of the fundamental mode in the reference or the sensing waveguide arm, respectively, Eq. (5) can be simplified as:

$$\frac{\Delta n_l}{\Delta \lambda_{dip}} \frac{\partial n_{eff}(s)}{\partial n_l} \lambda_{dip} L_s = [n_g(r) L_r - n_g(s) L_s] \tag{7}$$

where [n_g (r)L_r– n_g (s)L_s] is the OPD between the two arms. The sensitivity of the proposed MZI sensor is defined as $\Delta \lambda_{dip} / \Delta n_l$, which thus can be obtained from Eq. (7) and expressed as:

$$S = \frac{\Delta \lambda_{dip}}{\Delta n_l} = \frac{\lambda_{dip}}{[n_g(r) L_r - n_g(s) L_s]} \frac{\partial n_{eff}(s)}{\partial n_l} L_s \tag{8}$$

In addition, free spectral region (FSR) of our proposed MZI can be derived as:

$$FSR = \frac{\lambda^2}{[n_g(r) L_r - n_g(s) L_s]} \tag{9}$$

Eq. (8) clearly reveals that the sensitivity is not only related to the sensing arm but also to the reference arm, and inversely proportional to the value of the OPD between the two arms of the used MZI, which means that, for the fixed waveguide materials and dimensions as well as a fixed sensing arm length, the sensitivity can be enhanced significantly by optimizing the reference arm length to reduce the OPD. It should be pointed out that the OPD between the two arms can also be reduced by engineering the waveguide dimensions to reduce the difference between the group effective RIs of the two waveguide arms of the used MZI, and with this method, temperature sensor with enhanced sensitivity has been demonstrated in [20]. In addition, according to Eq. (8) the sensitivity can even approach infinity when the value of the OPD is close to zero. This, however, will also cause the FSR to approach infinity. In practice, such a large FSR requires not only an expensive ultra-broadband light source for the sensing system but also a high-precision design and fabrication technology to realize a very high extinction required for the trace of the dip wavelength in the transmission spectra accurately, both lead to high costs. Thus to implement our proposed cost-effective MZI sensor, it is necessary to balance the FSR and the sensitivity by choosing a suitable L_r to obtain a suitable value of the OPD.

To investigate numerically the sensitivity of the proposed MZI sensor and then design the key parameters of the device, we calculated the value of the OPD and the sensitivity for different L_r from 7900.0 to 7980.0 μm by considering the MZI with aforementioned reference and sensing waveguide dimensions and assuming $L_s = 7900.0$ μm, $\lambda_{dip} = 1550$ nm, and ignoring material dispersion. Note that here $n_g(r)$ is smaller than $n_g(s)$ for the waveguides with different widths of $w_r = 2.5$ μm and $w_s = 2.0$ μm but with the same height of $h = 1.7$ μm. The calculated results for the TM polarization are shown in Fig. 2. It can be seen that with L_r increases from 7900.0 to 7980.0 μm the value of the OPD decreases linearly, while the sensitivity increases slowly at first and then sharply after the value of the OPD is less than 20. When $L_r = 7980.0$ μm, the value of the OPD approaches to zero and the achieved sensitivity is 9×10^4 nm/RIU, which has a ~17-fold enhancement, in comparison with the sensitivity of 5264.0 nm/RIU achieved with $L_r = 7900.0$ μm. It should be pointed out that the related values for the TE polarization were also calculated but they are inferior to the values for the TM polarization due to a somewhat weak evanescent field, thus for simplicity they are not shown here.

Although the calculated results above show that an ultra-high sensitivity of 9×10^4 nm/RIU can be attained when $L_r = 7980.0$ μm. However, the corresponding FSR is as large as 336.90

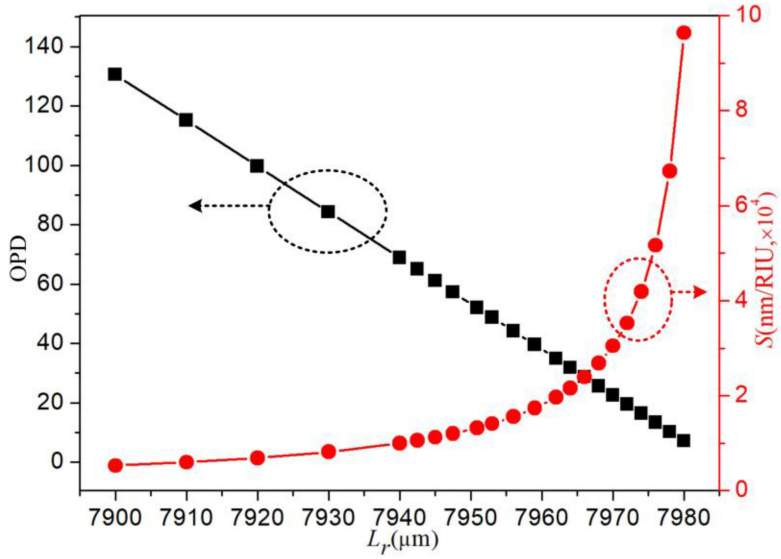

Fig. 2. The value of the OPD and the sensitivity (S) as a function of L_{r} when $L_{\mathrm{s}} = 7900.0$ μm, $w_{\mathrm{r}} = 2.5$ μm, $w_{\mathrm{s}} = 2$ μm, and $h = 1.7$ μm for the TM polarization.

nm, which is too large to realize a cost-effective MZI sensor as discussed above. In addition, the corresponding figure of Merit (FOM), used to evaluate the optical resolution and calculated as S/FWHM, is only 359/RIU, where FWHM is the full width at half maximum. Considering this situation as well as for comparison, we choose $L_{\mathrm{r}} = 7900.0$ (denoted as S_1), 7942.5 (S_2), 7950.9 (S_3), 7962.2 (S_4), and 7969.5 μm (S_5) while $L_{\mathrm{s}} = 7900.0$ μm in this work, corresponding to, respectively, theoretical sensitivities of 5264, 9983, 13210, 19867, and 29456 nm/RIU, and FOMs of 560, 538, 560, 562, and 566/RIU. Obviously, the sensitivities achieved by optimizing the OPD between the two arms are much larger than that achieved with the same arm lengths of $L_{\mathrm{r}} = L_{\mathrm{s}} = 7900.0$ μm (S_1). The detection range (DR) of our proposed MZI is given by

$$DR = \frac{FSR}{S} = \frac{2\pi}{\frac{\Delta\varphi}{\Delta n_l}} = \frac{\lambda}{L_s \frac{\partial n_{eff}(s)}{\partial n_l}} \tag{10}$$

where $\Delta\varphi$ is the change of the phase difference between the two arms, which is caused by the Δn_l and determined only by the sensing arm since the reference arm is isolated from the analyte in our proposed MZI configuration. Thus, for a fixed sensing arm, $\Delta\varphi$ is an constant, thus our proposed MZI sensor can enhance the sensitivity by optimizing the reference arm length while maintain a fixed DR. This is different from most sensitivity enhancement schemes in which the $\Delta\varphi$ is increased by enhancing the light-analyte interaction length or degree of the MZI sensor [11]–[14].

3. Results and Discussion

We followed the designed parameters to fabricate the proposed device. A 1.7 μm thick BCB film was first spin-coated on an oxidized silicon substrate having a 3.0 μm thick silica buffer. After the BCB layer was fully cured, the designed MZI pattern was realized by the standard photolithography and then transferred into BCB film by the inductively coupled plasma (ICP) etching with the mixture gases of Ar and CF_4. Subsequently, a PMMA film was spin-coated onto the sample to form the upper cladding. Finally, the sensing window was defined by the lithography process and the sensing area was exposed by the oxygen ICP etching process. It should be pointed out that the oxygen ICP etching process does little damage to the BCB waveguide formed previously because the etching rate for the PMMA is much faster than that for the BCB. For comparison, we fabricated the designed

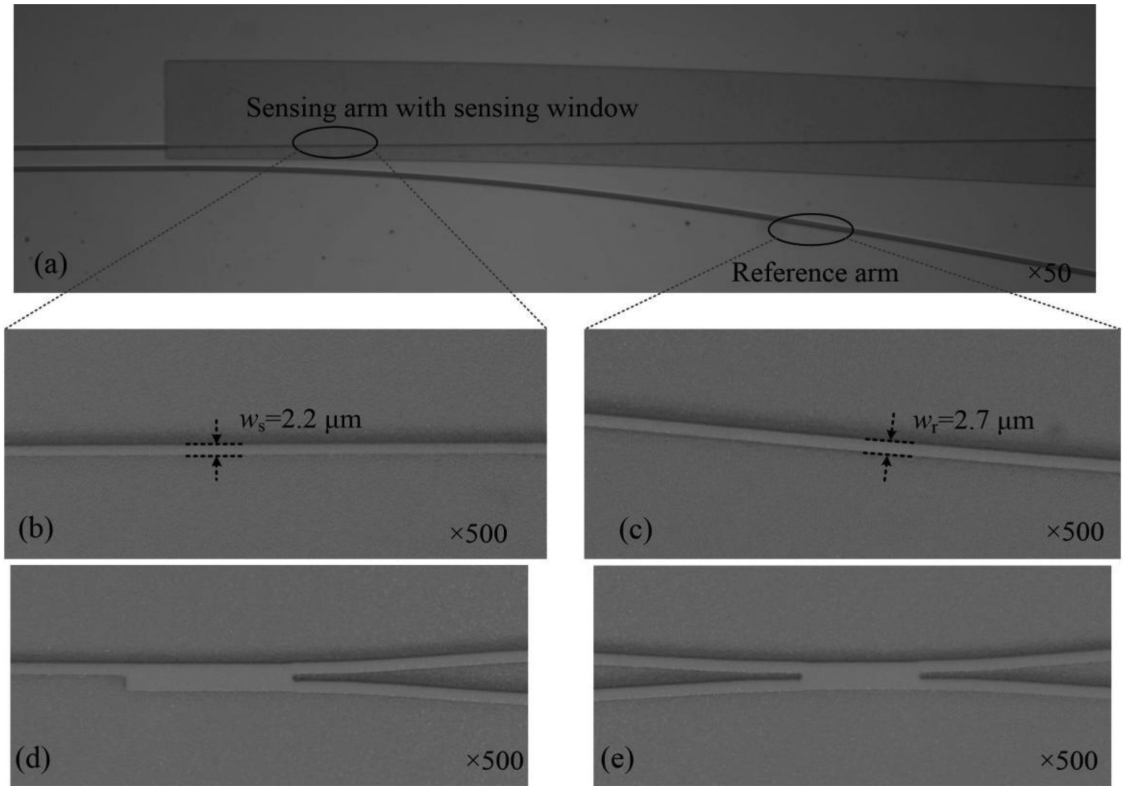

Fig. 3. Optical micrographs of (a) the sensing arm and reference arm of our fabricated MZI, (b) the sensing waveguide, (c) the reference waveguide, (d) input TMI, and (e) output TMI.

five MZI sensors (S_1-S_5) on the same sample. The optical micrographs of several important areas of the fabricated MZI at different objective multiples together with the measured width of the waveguide arms are shown in Figs. 3(a)–3(e). The widths of the two fabricated waveguide arms are $w_r = 2.7$ μm and $w_s = 2.2$ μm, respectively. The height of the fabricated waveguide, measured with a step profiler (Ambios XP-2), is 1.72 μm. Due to the unavoidable fabrication errors, the dimensions of the fabricated waveguides are slightly larger than those of designed. From Eq. (8), the change of the sensing and the reference waveguide dimensions has a complicated impact on the sensitivity of our proposed MZI sensor because it will lead to the changes of the waveguide sensitivity, the OPD, and the λ_{dip}. However, the calculated results show that the changes of 0.2 μm in width and 0.02 μm in height of the sensing and the reference waveguides will lead to the changes less than 10.7% in the sensitivity of our designed five MZI sensors, showing a moderate fabrication tolerance.

To characterize the fabricated sensors, the output light from an amplified spontaneous emission (ASE) light source (B&A, AS4600) was launched into Input waveguide of the MZI sensor via a lensed single-mode fiber (SMF). The output light signal from Output waveguide 1 or 2 was collected by an SMF and monitored by an optical spectrum analyzer (OSA) (Anristu MS97740A). An optical fiber online polarizer and a polarization controller (PC) were used to ensure that only TM polarized light was coupled into the sensor.

The sensitivity of the fabricated MZI sensors was investigated by measuring the transmission spectra at different liquid analyte concentration. The liquid analyte used in this work is sucrose solution with different concentrations of 0% (deionized water, DI water), 0.2%, 0.3%, 0.5%, 0.8%, and 0.9%. For the MZI sensors S_1, S_2, and S_3, the measured transmission spectra at different sucrose solution concentrations of 0%, 0.2%, 0.5%, 0.8%, and 0.9% are shown in Figs. 4(a)–4(c), respectively. The corresponding FSR of ∼20, ∼44, and ∼52 nm can be read out directly from these

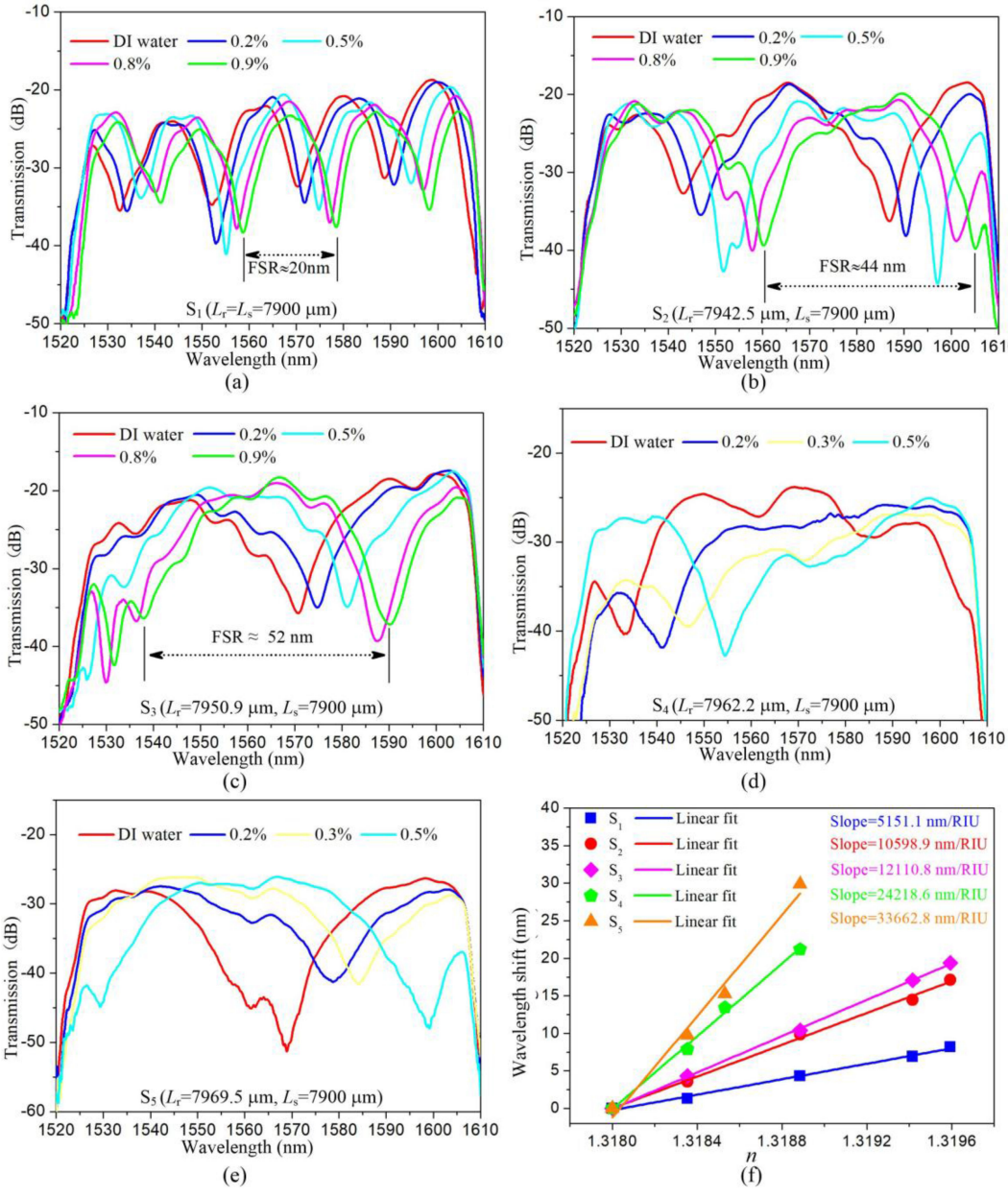

Fig. 4. Transmission spectra at different liquid concentration of our fabricated MZI sensors (a) S_1, (b) S_2, (c) S_3, (d) S_4, and (e) S_5. (f) Dip wavelength shifts versus the sucrose solution RI, linear fit are used to obtain the slopes ($R^2 = 0.99$).

three figures, which are in good agreement with the results that calculated using Eq. (9). For the MZI sensors S_4 and S_5, the measured transmission spectra at different sucrose solution concentrations of 0%, 0.2%, 0.3%, and 0.5% are shown in Figs. 4(d) and 4(e), respectively. Their FSR cannot be read out directly from Figs. 4(c) and 4(d) due to the limited bandwidth of our used ASE light source. It can be seen from Figs. 4(a)–4(e) that the concerned dips in transmission spectra of these five sensors exhibit an extinction ratio higher than 15 dB, which is enough for the readout of the wavelength shift. Also one can see that the concerned dips of these five MZIs red-shift with the increase in sucrose solution concentration but the dips corresponding to S_5 exhibit the largest shifts.

TABLE 1
Performances of Our Fabricated Five MZI Sensors

Sensor	L_r (μm)	L_s (μm)	FSR (nm)		Sensitivity (nm/RIU)		FOM (RIU^{-1})	DR (RIU)	
			Theory	Experiment	Theory	Experiment			
S_1	7900	7900	18	20	4388.4	5151.1	584	0.0039	0.0041±0.0002
S_2	7942.5		40	44	10157.4	10598.9	601	0.0041	
S_3	7950.9		51	52	12937.2	12110.8	573	0.0043	
S_4	7962.2		81	--	20475.1	24218.6	635	--	
S_5	7969.5		130	--	32834.2	33662.8	790	--	

TABLE 2
Comparison of the Sensitivity of Some MZI Sensors

MZI sensors	Sensitivity	References
Plasmonics co-integrated with silicon nitride photonics	1973 nm/RIU	[10]
Silicon nitride slot waveguide	2663π/cm RIU	[11]
double-slot hybrid plasmonic waveguide	1061 nm/RIU	[12]
hollow hybrid plasmonic waveguide	160 nm/RIU	[13]
Subwavelength grating slot waveguides	598.6 nm/RIU	[14]
Optical waveguide with metal under-cladding	5280 nm/RIU	[15]
Dip splitting effect	5×10^4 nm/RIU	[16]
Vernier effect	21500 nm/RIU	[18]
This work (L_r = 7969.5 μm, in experiment)	33662.8 nm/RIU	-
This work (L_r = 7980 μm, in theory)	9×10^4 nm/RIU	-

To obtain the sensitivities of the fabricated MZI sensors, we plotted the dip wavelength shifts versus the sucrose solution RI together with the linear fitting lines, which are shown in Fig. 4(f). The dip wavelengths almost linearly shift with the increase of the RI. Linear fitting lines show that the sensitivities of the fabricated MZI sensors S_1 - S_5 are 5151.1, 10598.9, 12110.8, 24218.6, and 33662.8 nm/RIU, respectively, which slightly differ from the theoretical results. This can be attributed to the errors in fabrication and measurement processes. Compared with the sensor S_1, the sensors S_2 – S_5 exhibit different degrees of enhancement in sensitivity, among which the sensor S_5 achieve a maximum enhancement of ~6.5-fold. These experimental results confirm obviously that the sensitivity of the MZI sensor can be enhanced significantly by just optimizing the reference arm length to reduce the OPD between the two arms of the MZI. In addition, we also calculated the DR of the sensors S_1, S_2, and S_3, based on Eq. (10) and using the FSRs read out from Figs. 4(a)–4(c), and the results are 0.0039, 0.0041, and 0.0043 RIU, respectively. Here, the DRs of the sensors S_4 and S_5 are not calculated since we can't read out the FSR of the two sensors from the transmission spectra. The DRs of these three sensors are slightly different, which is not because of the change in reference arm length, but is because of the errors in the processes of sensing measurement and data reading. Hence, these three MZI sensors have almost the same DR of 0.0041 ± 0.0002 RIU. Further, to evaluate the optical resolution, we also calculated the FOM of the fabricated MZI sensors S_1 - S_5, and the results are 584, 601, 573, 635, and 790/RIU, showing good optical resolutions. Table 1 summarizes the performances both in theory and in experiment of these five sensors.

For comparison, the sensitivities of some reported MZI sensors are summarized in Table 2. For the sensors using the novel waveguides to enhance sensitivity [10]–[15], the MZI sensor with silicon nitride slot waveguide achieved the sensitivity of 2633π/cm RIU [11], while the other MZI sensors in [10], [12]–[15] exhibit the sensitivity lower than that achieved in this work. For the sensors based on engineering the OPD of used MZI to enhance sensitivity [16], [18], the sensitivity of our proposed MZI sensor is much larger than that of the MZI sensor based on vernier effect in [18], but slightly inferior to the MZI sensor based on dip splitting effect in [16]. However, our proposed MZI sensor

has advantages of structural simplicity, easy processing, and mass fabrication capability and hence, is cost-effective. Moreover, based on the theoretical result, there should be some room to further enhance the sensitivity of our proposed sensor by optimizing the design of the MZI and improving the fabrication skill of the device.

4. Conclusion

In summary, by optimizing the reference arm length to decrease the OPD between the two arms of the proposed MZI, we demonstrated a cost-effective liquid RI sensor based on a simple MZI configuration formed with polymeric conventional strip waveguide. Our theoretical result exhibit the proposed MZI sensor can achieve the RI sensitivity of 9×10^4 nm/RIU. While our experimental sensor exhibits a high sensitivity of 33662.8 nm/RIU. Our proposed MZI sensor is cost-effective and could also be realized with other organic or inorganic waveguide materials.

Disclosures

The authors declare no conflicts of interest.

References

[1] X. Fan, I. M. White, S. I. Shopova, H. Zhu, J. D. Suter, and Y. Sun, "Sensitive optical biosensors for unlabeled targets: A review," *Anal Chim Acta*, vol. 620, no. 1/2, pp. 8–26, Jul. 2008.

[2] P. Liu and Y. Shi, "Simultaneous measurement of refractive index and temperature using a dual polarization ring," *Appl. Opt.*, vol. 55, no. 13, pp. 3537–3541, May 2016.

[3] W. Zhang, S. Serna, X. L. Roux, L. Vivien, and E. Cassan, "Highly sensitive refractive index sensing by fast detuning the critical coupling condition of slot waveguide ring resonators," *Opt. Lett.*, vol. 41, no. 3, pp. 532–535, Feb. 2016.

[4] Y. J. Wen *et al.*, "High sensitivity and FOM refractive index sensing based on fano resonance in all-grating racetrack resonators," *Opt. Commun.*, vol. 446, pp. 141–146, 2019.

[5] Q. Liu, Z. Gu, M. K. Park, and J. Chung, "Experimental demonstration of highly sensitive optical sensor based on grating-assisted light coupling between strip and slot waveguides," *Opt. Exp.*, vol. 24, no. 12, pp. 12549–12556, Jun. 2016.

[6] N. Saha and A. Kumar, "Toward 100 micrometer per refractive index unit sensitive sensor using a compact long-period grating inscribed metal clad ridge waveguide," *J. Lightw. Technol.*, vol. 36, no. 10, pp. 2024–2030, 2018.

[7] M. Wang *et al.*, "Highly sensitive biosensor based on UV-imprinted layered polymeric–inorganic composite waveguides," *Opt. Exp.*, vol. 20, no. 18, pp. 20309–20317, Aug. 2012.

[8] M. Kumar, A. Kumar, and R. Dwivedi, "Ultra high sensitive integrated optical waveguide refractive index sensor based on multimode interference," *Sensors Actuators B: Chem.*, vol. 222, pp. 556–561, 2016.

[9] K. Misiakos *et al.*, "Broad-band Mach-Zehnder interferometers as high performance refractive index sensors: Theory and monolithic implementation," *Opt. Exp.*, vol. 22, no. 8, pp. 8856–8870, Apr. 2014.

[10] A. Manolis *et al.*, "Plasmonics co-integrated with silicon nitride photonics for high-sensitivity interferometric biosensing," *Opt. Exp.*, vol. 27, no. 12, pp. 17102–17111, Jun. 2019.

[11] Q. Liu *et al.*, "Highly sensitive Mach–Zehnder interferometer biosensor based on silicon nitride slot waveguide," *Sensors Actuators B: Chem.*, vol. 188, pp. 681–688, 2013.

[12] X. Sun, D. Dai, L. Thylen, and L. Wosinski, "High-sensitivity liquid refractive-index sensor based on a Mach-Zehnder interferometer with a double-slot hybrid plasmonic waveguide," *Opt. Exp.*, vol. 23, no. 20, pp. 25688–25699, Oct. 2015.

[13] X. Sun, L. Thylén, and L. Wosinski, "Hollow hybrid plasmonic Mach–Zehnder sensor," *Opt. Lett.*, vol. 42, no. 4, pp. 807–810, 2017.

[14] M. Odeh, K. Twayana, K. Sloyan, J. E. Villegas, S. Chandran, and M. S. Dahlem, "Mode sensitivity analysis of subwavelength grating slot waveguides," *IEEE Photon. J.*, vol. 11, no. 5, Oct. 2019, Art. no. 2700210.

[15] R. Dwivedi and A. Kumar, "A compact and ultra high sensitive RI sensor using modal interference in an integrated optic waveguide with metal under-cladding," *Sensors Actuators B: Chem.*, vol. 240, pp. 1302–1307, 2017.

[16] R. Levy, S. Ruschin, and D. Goldring, "Critical sensitivity effect in an interferometer sensor," *Opt. Lett.*, vol. 34, no. 19, pp. 3023–3025, Oct. 2009.

[17] R. Levy and S. Ruschin, "Critical sensitivity in hetero-modal interferometric sensor using spectral interrogation," *Opt. Exp.*, vol. 16, no. 25, pp. 20516–20521, Oct. 2008.

[18] X. Jiang, Y. Chen, F. Yu, L. Tang, M. Li, and J. J. He, "High-sensitivity optical biosensor based on cascaded Mach-Zehnder interferometer and ring resonator using vernier effect," *Opt. Lett.*, vol. 39, no. 22, pp. 6363–6366, Nov. 2014.

[19] G. M. Hale and M. R. Querry, "Optical constants of water in the 200-nm to 200-μm wavelength region," *Appl. Opt.*, vol. 12, no. 3, pp. 555–563, 1973.

[20] Y. Zhang, J. Zou, and J. J. He, "Temperature sensor with enhanced sensitivity based on silicon Mach-Zehnder interferometer with waveguide group index engineering," *Opt. Exp.*, vol. 26, no. 20, pp. 26057–26064, Oct. 2018.